Effects of material properties on the competition mechanism of heat transfer of a granular bed in rotary cylinders*

Xie Zhi-Yin(谢知音) and Feng Jun-Xiao(冯俊小)†

School of Mechanical Engineering, University of Science and Technology Beijing, Beijing 100083, *China*

(Received 26 September 2012; revised manuscript received 17 December 2012)

Mixing and heat transfer processes of the granular materials within rotary cylinders play a key role in industrial processes. The numerical simulation is carried out by using the discrete element method (DEM) to investigate the influences of material properties on the bed mixing and heat transfer process, including heat conductivity, heat capacity, and shear modulus. Moreover, a new Péclet number is derived to determine the dominant mechanism of the heating rate within the particle bed, which is directly related to thermal and mechanical properties. The system exhibits a faster heating rate with the increase of ratio of thermal conductivity and heat capacity, or the decrease of shear modulus when inter-particle conduction dominates the heating rate; conversely, it shows a fast-mixing bed when particle convection governs the heating rate. The simulation results show good agreement with the theoretical predictions.

Keywords: rotary cylinder, particle mixing, heat conduction, material properties

PACS: 45.70.–n, 44.10.+i, 44.30.+v **DOI:** 10.1088/1674-1056/22/8/084501

1. Introduction

The mixing and heat transfer processes of particle materials within rotary cylinders are important in industrial applications, such as heating, cooling, and calcinations. It is important to understand the mixing characteristics and heat transfer performance. However, the influences of the material properties on mixing and heat transfer process, which have significant effects on the dominant mechanism of the heating rate, have not been systematically investigated yet. Heat conduction is determined by particle–particle or particle–wall contacts and affected by many factors.[1] Based on the thermal particle dynamics, the effects of both mechanical and thermal information in a two-dimensional (2D) packed bed of particles were investigated.[2] Schlünde[3] reported that heat conduction through particle contact is dominated when particle diameter is very small (< 1 mm). And he defined a concept of particle convection, which is similar to fluid flows, to describe particle flows. Particles are in densely packed in a moving bed, which provides a longer contact time with a much smaller fraction of voids compared with a fluid bed.[4] Therefore, the contact conduction will be the dominant mechanism of the heat transfer in the particle bed within rotary cylinders. Boateng and Barr[5] deveploped a mathematical model to predict heat transfer from the freeboard gas to the bed, temperature distribution within the bed, and the refractory wall at any axial position of the kiln. Van Puyvelde *et al.*[6] reported that mixing rate increases linearly with filling degree by image analysis based on experiment study. Liu and Eckehard[7] measured the temperature distribution in a moving bed in a pilot kiln by a thermal couple array.

Kwapinsk *et al.*[8] investigated the particle motion in the transaction of a 2D rotary drum by discrete element method (DEM) simulation, based on the previous experiments and the definition of the bed rotation speed. Liu *et al.*,[9] and Zhao and Cheng[10] studied the mixing process of a binary particle system in the rotary durm. Shi *et al.*[11] combined the DEM and computational fluid dynamics (CFD) to investigate the overall heat transfer process in a rotary kiln in order to find the transition criteria from convection-dominated process to conduction-dominated process. Bodhisattwa *et al.*[12] simulated the particle flow and particle–wall heat transfer in calciners and impregnators by varying material properties, and the effects of thermal properties of granular material have been analyzed. The heat convection of the particle group caused by the mixing effect may be dominant[13] according to relatively small conductivity of bed material in industrial applications.

In the direct-fire rotary kiln, particles in the upper layer are first heated by flame radiation, then mix with the cooler particles in the active layer as the heat transfer medium.[14] Therefore, the particle mixing phenomenon of the upper and lower layers should be focused upon, however, the relevant reports are rare. The effects of operational parameters on particle mixing and heat transfer performance have been done in our previous work (submitted to a journal), and the effects of thermal and mechanical properties on heat transfer performance will be investigated in the present paper.

To obtain the information about particle mixing and heat transfer in particle level, experiments in this field are often

*Project supported by the National High Technology Research and Development Program of China (Grant No. 2007AA05Z215) and the Fundamental Research Funds for the Central Universities (Grant No. FRF-AS-10-005B).

†Corresponding author. E-mail: jxfeng@ustb.edu.cn

© 2013 Chinese Physical Society and IOP Publishing Ltd

of limited applicability due to their high cost. Alternatively, DEM has been increasingly accepted as an effective tool to investigate the heat transfer phenomena in particulate systems. Therefore, the thermal DEM will be employed to study the particle mixing and heat transport process within rotary cylinders by varying material properties of particles, including thermal conductivity k_s, heat capicity c_p, and Young modual G. Moreover, a new Péclet number will be introducted to describe the competition between thermal diffusion of particle bed and bed mixing rate on heating rate. The influences of the three parameters on heat transfer performance will be systematically investigated to determine the predominant mechanism of heat transfer process.

2. Modeling of particle dynamic and heat transfer

2.1. Governing equations of particles

The discrete element model has been widely used to investigate granular behaviors recently, and often used to replace or implement the experimental research.[15] It was first developed by Cundall and Strack[16] in the 1970s. The translational and rotational motions of a particle of radius R_i and mass m_i can be described as

$$m_i \frac{\mathrm{d}v_i}{\mathrm{d}t} = \sum_j (F_{ij}^{\mathrm{n}} + F_{ij}^{\mathrm{s}} + m_i g), \tag{1}$$

$$I_i \frac{\mathrm{d}\omega_i}{\mathrm{d}t} = \sum_i (R_i \times F_{ij}^{\mathrm{s}} - \mu_{\mathrm{r}} R_i \left|F_{ij}^{\mathrm{n}}\right| \hat{\omega}_i). \tag{2}$$

Here, v_i, ω_i, and I_i represent the translational, angular velocities, and moment of inertia of the particle respectively, R_i is a vector ranging from the center of the particle to the contact point, F_{ij}^n and F_{ij}^{s} are the normal contact force and the tangential contact force acting on particle i by particle j, respectively, u_{r} is the rolling friction coefficient, g the gravity acceleration, and m_i the mass of particle i.

The Hertz-Mindle model with no slip — a more accurate and proper mathematical model for particle contact – was obtained.[17] The elastic constant is a function of geometrical and physical properties of the particle and wall as

$$K_n = \frac{4}{3} E_{\mathrm{eq}} \sqrt{R_{\mathrm{eq}}}. \tag{3}$$

Here, E_{eq} and R_{eq} are the equivalent Young's modulus and equivalent radius respectively. The relation between normal force f_{n} and noraml displacement δ_{n} can be expressed as

$$f_{\mathrm{n}} = -K_{\mathrm{n}} \cdot \delta_{\mathrm{n}}^{3/2}. \tag{4}$$

The micro-slip phenomenon is negelected, the tangential force is evaluated as

$$f_{\mathrm{n}} = -K_{t0} \cdot \delta_t. \tag{5}$$

Here, K_{t0} is the initial stiffness constant, which is a function of equivalent shear modulus G_{eq}, radius R_{eq}, and actual normal displacement δ_{n}, and expressed as

$$K_{t0} = 8 G_{\mathrm{eq}} \sqrt{R_{\mathrm{eq}} \delta_{\mathrm{n}}}. \tag{6}$$

Hertz–Mindle (no slip) model can provide more details at the microscopic scale.[17] The time step should be short enough, which is about 10^{-5} s $\sim 10^{-7}$ s, according to the mechanical property in this work.[18]

2.2. Heat transfer model

2.2.1. Conduction model

Thermal conduction within the solid particle and through the contact area between two particles is only of concern in this system. And conduction is expected to be dominant while the interstitial gas is stagnant with a much smaller thermal conductivity compared with the particle material. This assumption can be valid when $k_s a / k_f \gg 1$,[19] where a is the contact radius, r is the particle radius of curvature, k_f represents the conductivity of interstitial gas, and k_s is the thermal conductivity of the particle material.

The thermal particle dynamics (TPD) is adopted as the basic model for thermal DEM.[20] The heat flow passes through the contact area of two particles i and j in contact, and the heat quantity between these two particles is:

$$Q_{ij} = H_{\mathrm{C}}(T_j - T_i). \tag{7}$$

The conductance can be calculated from Hertz contact theory as

$$H_{\mathrm{C}} = 2k_{\mathrm{s}} \left[\frac{3F_N R_{\mathrm{eq}}}{4E_{\mathrm{eq}}}\right]^{1/3}. \tag{8}$$

If the temperature gradients are confined to the contact area, the conduction resistance within the particle is smaller than between the particles, which can serve as Biot number. Vargas and McCarthy[20] have derived the Bi on solid conduction as

$$Bi = \frac{H_{\mathrm{c}} R}{k_{\mathrm{s}} A} = \frac{2ak_{\mathrm{s}} R}{k_{\mathrm{s}} A} = \frac{2aR}{\pi R^2} = \frac{2}{\pi}\sqrt{\frac{\alpha}{R}}. \tag{9}$$

Here, $a = \sqrt{R\alpha}$ represents the contact radius, and α is the computational overlap of contacting particles. Because $\alpha \ll R$, we can conclude that $Bi \ll 1$. This implies that the resistance to heat transfer inside a particle is significantly smaller than between interacting particles.

The evolution of the temperature of particle i when contacting particle j is given as

$$\frac{\mathrm{d}T_i}{\mathrm{d}t} = \frac{Q_i}{\rho_i c_i V_i}. \tag{10}$$

Here, T_i is the temperature of particle i , Q_i the total amount of heat quantity transferred to particle i from its neighbor (particle j), ρ_i the density of material of particle i, c_i the heat capacity of particle i, and V_i the volume of particle i.

Then the temperature of particle i, T_i, at time $t+\Delta t$ can be calculated from

$$T_i^{t+\Delta t} = T_i^t + \sum_{j=1}^{N} \Delta T_{ij}^{t+\Delta t} = T_i^t + \sum_{k=1}^{N} \left(T_j^t - T_i^t\right)\left(1-\exp\left[-\frac{H_c}{\rho_i c_i V_i}\right]\Delta t\right). \quad (11)$$

Equations (7), (8), (9), and (10) can be used to calculate the temperature variation of each particle in the material bed. In addition, the material properties remain unchanged and the wall of rotating cylinder is adiabatic.

2.2.2. Effective thermal conductivity

The effective thermal conductivity (ETC) for two contacting particles within a packed bed has been described with the consideration of many correlations.[21] For pure conduction, Batchelor and O'Brien[19] have proposed independently the approximate analytical solutions of heat conductance, which is presented as Eq. (8). And Zhang *et al.*[22] used the simple cubic arranged granular assemblies to investigate the particle size effect on the overall thermal conduction properties, and reported that the ETC is inversely proportional to particle diameter. Therefore, the ETC for a packed bed can be turned into

$$k_e = \frac{2k_s}{d_P}\left(\frac{3F_N R_{eq}}{4E_{eq}}\right)^{1/3}. \quad (12)$$

Then, a certain k_e of the packed bed can be obtained by simulations under a constant void fraction.[20] However, it is much more complicated when this two-particle model is extended to a moving bed within rotary cylinders, which is rarely studied at present. First, it is a complex function affected by material properties, including shear modulus, thermal conductivity, heat capacity, particle diameter and distribution, void fraction, coordinate number distribution, and normal force distribution, and so on. Second, there is no equilibrium state to determine k_e for a rotation bed, compared with for the packed bed. Considering the focus of this research, the attention should be paid to the effects of the material properties. Thus, a fitting parameter ξ is introduced to simplify the above multiple effects, and some parameters are listed in Table 1. Then, the ETC for the moving bed can be simplified into

$$k_e = \frac{2\xi k_s}{d_P}\left(\frac{3F_N R_{eq}}{5.6G}\right)^{1/3}. \quad (13)$$

3. Mixing dynamics

3.1. Mixing rate analysis

The mixing process is used to make a better temperature distribution within the kilns, and maintain a high temperature difference of mixing particles in the active layer to achieve good heat transfer efficiency. The radial mixing, which is much faster than axial mixing, is concerned with its complexity depending strongly on both filling degree and rotation speed of rotary kilns. By intoducing the definition of the bed rotation speed,[23] Kwapinsk[8] developed an updated model of the mixing number and cylinder revolution based on the model derived by Schlünder and Mollekopf[24] in their contact experiments. It has been validated by the previous experiments[4] as

$$N_{mix} = 4.52 Fr'^{0.22}. \quad (14)$$

Here, N_{mix} is the mixing number, which refers to the revolutions of the rotating cylinder when particle bed reaches a perfect mixing state, and Fr' is the Froude number of the particle bed and expressed as

$$Fr' = \frac{(2\pi n')^2 D}{2g}. \quad (15)$$

Here, D is the diameter of the rotary cylinder, and n' the bed rotation speed, which can be presented as

$$n' = \frac{2\pi n}{\theta}. \quad (16)$$

Here, θ is the cover angle of particle bed.[23] Moreover, the filling degree f can be calculated by the chord area obtained by the bed cover angle θ. Thus, the relation between the filling degree and the bed cover angle is gained by data regression:

$$f = 0.0167\theta^2 + 0.1067\theta + 0.0023. \quad (17)$$

Then, equation (14) can be derived as

$$N_{mix} = 6.02\left(\frac{n}{\theta}\right)^{0.44}. \quad (18)$$

It can be seen that the mixing number N_{mix}, as well as mixing rate $1/t_R$, is strongly affected by both filling degree and rotation speed of rotary kilns. The mixing time can be obtained from $t_R = N_{mix}/n$,[8] then, the mixing rate can be defined as

$$\frac{1}{t_R} = 0.019 n^{0.56} f^{0.4}. \quad (19)$$

3.2. Heating rate analysis

The mechanism of heat transfer process in particle bed within the rotary cylinder is complicated. It implies that the inter-particle conduction and particle mixing are alternately dominated under different conditions. The heat conduction occurs only between two contacting particles, and the energy transferring through the contact area depends on not only the size of the contact area, but also the duration of the contact and material properties. Consequently, the mechanical and thermal properties will affect the heat conductive or diffusive rate through the particles. On the other hand, the particle convection, caused by the bed rotation, will also affect the heating rate, where mass transfers from a hotter region to a colder one.

In this work, the Péclet number will be used to determine the dominant mechanism in the overall bed heating.[13] A new Péclet number for particulate system is defined as follows:

$$Pe = \frac{\text{mixing rate}}{\text{rate of thermal diffusion}} = \frac{1/t_R}{\alpha/l^2}, \tag{20}$$

where $1/t_R$ has been defined in Subsection 3.1; α is the effective thermal diffusivity of the particle bed, which is related to the thermal property of particle material; l is the characteristic length of the system, which is set to be the equivalent diameter of the rotary kiln. Therefore, $\alpha = k/c_p\rho$, where conductivity $k = k_e$, density $\rho = \rho_s(1-\varepsilon)$, k_e being the effective thermal conductivity of particle material, which is given in Eq. (14), ε the average void fraction of particle bed. Then, the Péclet number can be derived as

$$Pe = \frac{\xi l^2 c_s \rho_s d_P (1-\varepsilon)}{2 t_R k_s} \left(\frac{5G}{3F_N R_{eq}}\right)^{-1/3}. \tag{21}$$

Equation (21) shows that the ratio of the thermal properties c_s/k_s, mechanical property G, and the mixing rate $1/t_R$ all determine the Péclet number.

Additionally, the equilibrium state should be defined as $Pe = 1$, which indicates that the heat transfer process is finished when bed mixing reaches a perfect state at the mixing time t_R, or the rotary cylinder reaches the revolutions of the mixing number N_{mix}. As shown in Fig. 1, the heat transfer process is considered to be finished, when temperature variation rate is smaller than 0.2 K/s, which is rather smaller than overall temperature cooling rate.

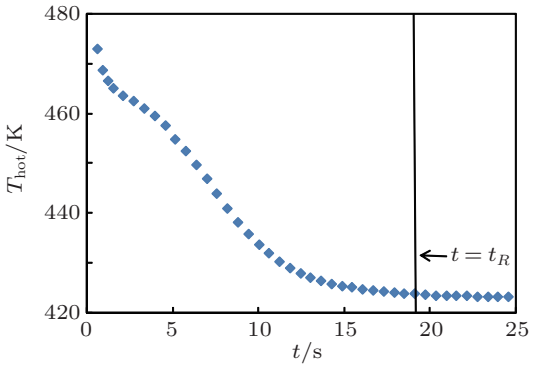


Fig. 1. (color online) Definition of equilium state when cooling process finishes at the mixing time t_R.

4. Results and analysis

Rotary cylinders filled by two kinds of spherical particles at different temperatures are simulated by a DEM program. Simulation conditions are summarized in Table 1. Considering the end plate effect, the both sides of cylinder end plates are set as periodic boundary condition (PBC). Therefore, the length of the rotary cylinder can be minimized to $L = 5.3d_P$, according to the simulations.[25,26] The rotation speed $n = 12.85$ rpm, which is in the rolling regime.

Table 1. Simulation condition and parameters.

Parameter	Value
Rotary cylinder, $D \times L$ (mm)	1000×80
Filling degree, f	40%
Rotation speed, n/rpm	12.85
Particle size, d_P/mm	15
Total number of particles, N	2000∼8000
Particle density/(kg/m^3)	3500
Specific heat, C_p/(J/kg·K)	25
Thermal conductivity, k_s/(W/m·K)	250∼1000
Particle size distributions	normal distribution 12 (0.8,1.2)
Shear modulus of particle/(N/m^2)	$10^7 \sim 10^9$
Poisson's ratio of particle and wall	0.29
Shear modulus of wall/(N/m^2)	1×10^8
Coefficient of restitution	0.6
Coefficient of static friction	0.5
Coefficient of rolling friction	0.005
Time step Δt	5×10^{-6}

For Eq. (20), mixing rate is governed by operational parameters. Based on the definition of the mixing time and the mixing number in Kwapinska's research,[8] the optimal mixing time is calculated to be $t_R = 18.1$ s, with corresponding mixing number $N_{mix} = 3.86$. The normal force F_N and void fraction ε are given as the average values of particle bed. And $l = 1000$ mm, according to geometry of the rotary cylinder. Thus, the effect of material properties on the Péclet number can be directly seen as

$$Pe = \frac{74 c_s G^{-1/3}}{k_s}. \tag{22}$$

Equation (22) shows the theoretical relation between Péclet number and the ratio of conductivity to heat capacity, shear modulus and Péclet number. Then, for the given optimal parameters, the Péclet number will be discussed under different material properties, to determine the dominant mechanism of heat transfer process in particle bed.

4.1. Effects of thermal properties

The thermal properties mainly include thermal conductivity and heat capacity. The heat conduction occurs in a limited contact area of the interface for two neighboring particles. Consequently, the conductivity of particle material can directly affect the rate of heat transfer. Similarly, the heat capacity is another important parameter, which demonstrates the temperature sensitivity of particles.

It can be predicted from Eq. (22) that $Pe < 1$ when $k_s/c_p < 43$ under the condition of the fixed $G = 1.0 \times 10^8$ N/m^2. Thus, the particle convection (or mixing effect) caused by cylinder rotation can be the predominant mechanism of the cooling process. In contrast, $Pe > 1$ when $k_s/c_p > 43$, then the inter-particle conduction governs the heating rate.

Figure 2 shows the effects of different values of k_s/c_p on heat transfer performance. Two parts of particles with a temperature difference gradually mix and the interface begin to

elongate, which provides more paths for enhancing the cooling rate. Both the conductivity and heat capacity determine the cooling rate, which contribute to faster heat diffusion with higher value of k_s/c_p.

With the increase of k_s/c_p, the temperature uniformity gradually increases at $t = 10.34$ s. But there is no further improvement at $t = 19.68$ s, relatively large temperature differences still exist in upper and bottom layers, which is caused by inadequate mixing. Therefore, it should be avoided in industrial process, and some effective measurements should be carried out, such as adding buffles at inner wall of rotary cylinders.

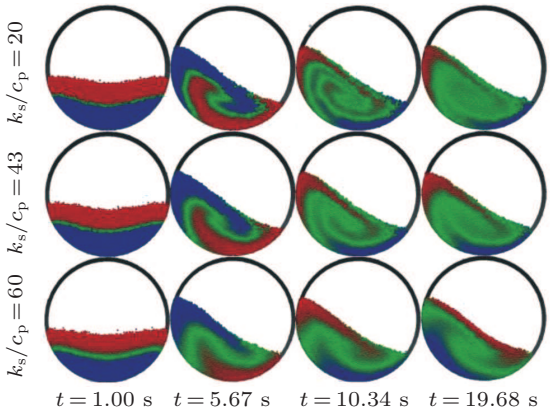


Fig. 2. (color online) Effects of k_s/c_p on the paritcle mixing and heat transfer process in rotary cylinder over time.

Figure 3 shows the temperature variations of hot particles with time for three values of k_s/c_p. When $k_s/c_p = 20$, the average temperature of hot particles T_{hot} continues to decline to an equilibrium state when time overpasses $t_R = 18.1$ s. Therefore, the cooling process lags behind the mixing process, which indicates the particle mixing mechanism is dominant for the heat transfer process. When $k_s/c_p = 43$, T_{hot} reaches the equilibrium state at about $t_R = 18.1$ s, which means that two mechanisms both control the cooling process. When $k_s/c_p = 60$, T_{hot} reaches the equilibrium state before the mixing time, which means that the cooling process overpasses the mixing process, and inter-particle conduction governs the heat transfer process. Consequently, different values of ratio k_s/c_p can determine the governing mechanism of cooling process of particle bed, and the above descriptions are well consistent with the prediction of Eq. (22).

To gain an insight into the evolutions of average temperature of hot particles T_{hot} within five revolutions, the values of T_{hot} in all time intervals are scaled by the average value at five revolutions. The results are illustrated in Fig. 4, showing that the smaller value of k_s/c_p makes cooling rate slower. At beginning, the case of $k_s/c_p = 60$ presents a larger decreasing rate, then $T_{avg}/T_{_5revs}$ dramatically declines and tends to flat at about 3 revolutions. Thus, $T_{avg}/T_{_5revs}$ can directly reflect the evolution of the cooling process. As $k_s/c_p = 43$, $T_{avg}/T_{_5revs}$ continues to decrease at 3 revolutions and tends to flat at $N_{mix} = 3.86$ revolutions. However, it keeps decreasing over 5 revolutions for the case of $k_s/c_p = 20$, which indicates that the heat transfer process is not finished yet, more revolutions are needed in order to achieve the temperature uniformity in the bed. The iron ore pellet ($k_s = 10$ W/m^2·K, $c_p = 2000$ J/kg·K) is taken as an example for the metallurgical industry process, and the result shows that its heat transfer process is far behind that with the mixing process.

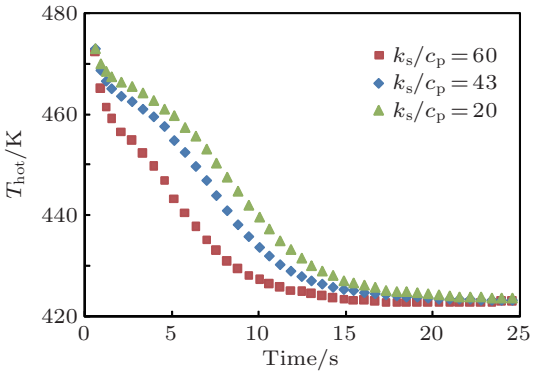


Fig. 3. (color online) Variations of average temperature of the hot particles with time for three values of k_s/c_p.

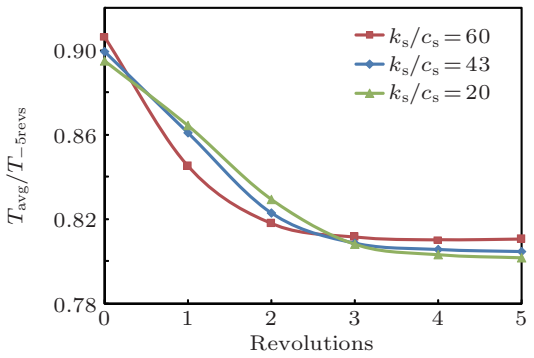


Fig. 4. (color online) Growths of scaled average bed temperature for varying k_s/c_p.

4.2. Effects of shear modulus

The shear modulus of particle material can strongly affect the size of the contacting area, according to the Hertz contact theory. Therefore, it can directly affect the inter-particle conduction and entire performance of the particulate system. Theoretically, the ETC of particle bed can decrease with shear modulus G in power function, according to Eq. (14). It can be predicted from Eq. (22) that $Pe < 1$ when $G < 1.0 \times 10^8$ N/m^2 under the condition of $k_s/c_p = 43$. Thus, the particle convection caused by bed rotation can be the governing mechanism of the cooling process. In contrast, $Pe > 1$ when $G > 1.0 \times 10^8$ N/m^2, then the inter-particle conduction governs the heating rate.

Figure 5 shows the effects of different shear moduli on heat transfer performance. Obviously, smaller shear modulus makes contact area larger, which attributes to faster heat diffusion. The interface gradually extends, which is caused by bed mixing at $t = 5.67$ s. It shows that a faster diffusive rate has a smaller shear modulus G. With the increase of G, the temperature uniformity gradually decreases at $t = 10.34$ s.

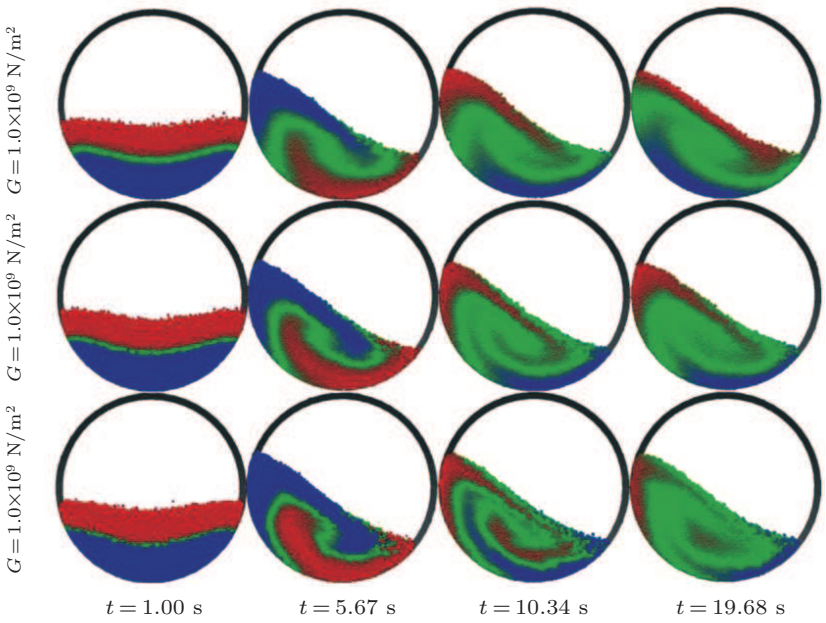


Fig. 5. (color online) Eeffects of shear modulus on paritcle mixing and heat transfer process in rotary cylinder over time.

Figure 6 shows the temperature variations of hot particles for different shear moduli. When $G = 1.0 \times 10^9$ N/m^2, the average temperature of hot particles T_{hot} continues to decline to reach an equilibrium state when time overpasses $t_R = 18.1$ s. Thus, the cooling process lags behind the mixing process, which indicates the heat transfer process is dominated by particle mixing mechanism. When $G = 1.0 \times 10^8$ N/m^2, T_{hot} reaches the equilibrium state at about $t_R = 18.1$ s, which implies that both mechanisms can control the cooling process. When $G = 1.0 \times 10^7$ N/m^2, T_{hot} reaches the equilibrium state before the mixing time t_R. Thus, it means that the cooling process will overpass the mixing process, and the inter-particle conduction will govern the heat transfer process. It can be concluded that different shear moduli can also determine the governing mechanism of cooling process, and the above descriptions are well consistent with the prediction of Eq. (22).

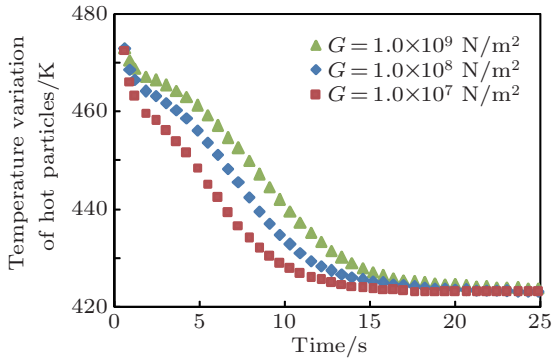


Fig. 6. (color online) Temperature variations of hot particles for varying shear modulus.

Similarly, the values of T_{hot} in all time intervals are scaled by the average value at five revolutions. The results shown in Fig. 7 indicate that the case of $G = 1.0 \times 10^7$ N/m^2 presents a larger decreasing rate at the beginning, then $T_{\text{avg}}/T_{_5\text{revs}}$ dramatically drops off and tends to flat at about 3 revolutions. As $G = 1.0 \times 10^8$ N/m^2, $T_{\text{avg}}/T_{_5\text{revs}}$ tends to flat at $N_{\text{mix}} = 3.86$ revolutions. However, it keeps decreasing over 5 revolutions for the case of $G = 1.0 \times 10^9$ N/m^2, which suggests that the heat transfer process is not finished yet, more revolutions are needed to achieve the temperature uniformity in the bed.

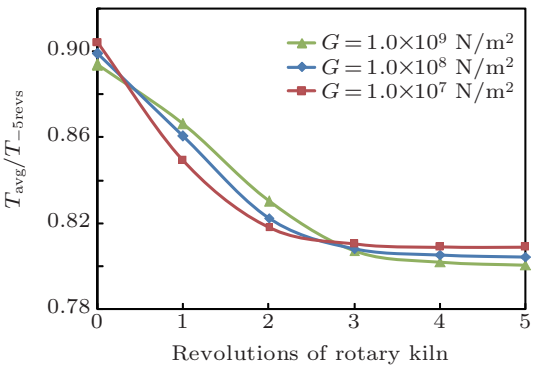


Fig. 7. (color online) Growths of scaled average bed temperature for varying shear modulus.

5. Conclusions

DEM is employed to examine the particle mixing and heat transfer process in three-dimensional rotating cylinders; the influences of the thermal properties and shear modulus are investigated. The system exhibits faster heating rate when the ratio of thermal conductivity to heat capacity increases or the shear modulus decreases. Additionally, the Péclet number is proposed to determine the dominated mechanism of heat transfer process within particle bed. The simulation results show good agreement with the theoretical predictions of the mechanism with different material properties. Fast-heating beds can

be obtained when $Pe > 1$ due to the higher value of k_s/c_p and lower value of shear modulus G, where the heating rate is dominated by heat conduction. In contrast, it is fast-mixing beds when $Pe < 1$ due to the lower vaule of k_s/c_p and higher value of shear modulus G; where the heat transfer process is governed by bed mixing.

References

[1] Vargas W L and McCarthy J J 2002 *Int. J. Heat Mass Transfer* **45** 4847
[2] Vargas W L and McCarthy J J 2002 *Chem. Eng. Sci.* **57** 3119
[3] Schlünde E U 1982 *Heat Transfer, Proc. 7th Int. Heat Transfer Conference*, Hemisphere Publishing Corporation **1** 195
[4] Moleurs Otto 1997 *Int. J. Heat Mass Transfer* **40** 4151
[5] Boateng A A and Barr P V 1996 *Int. J. Heat Mass Transfer* **39** 2131
[6] van Puyvelde D R, Young B R, Wilson M A and Schmidt S J 1999 *Powder Tech.* **106** 183
[7] Liu X Y and Eckehard S 2010 *Chem. Eng. Process.* **49** 147
[8] Kwapinska M, Saage G and Tsotsas E 2006 *Powder Tech.* **161** 69
[9] Liu Y L, Zhang X Q and Zhao Y Z 2009 *Acta Phys. Sin.* **58** 8386 (in Chinese)
[10] Zhao Y Z and Cheng Y 2008 *Acta Phys. Sin.* **57** 322 (in Chinese)
[11] Shi D S, Vargas W L and McCarthy J J 2008 *Chem. Eng. Sci.* **63** 4506
[12] Bodhisattwa C, Fernando J, Muzzio M and Silvina T 2006 *Chem. Eng. Sci.* **61** 6348
[13] Isabel F, Vargas W L and McCarthy J J 2010 *Chem. Eng. Sci.* **65** 1045
[14] Xie Z Y and Feng J X 2013 *J. Central South Univ. Tech.* (In Press)
[15] Thornton C and Antony S.J 2000 *Powder Tech.* **109** 179
[16] Cundall P A and Strack O D L 1979 *Geotechnique* **29** 47
[17] Alberto D R and Francesco P D M 2004 *Chem. Eng. Sci.* **59** 525
[18] Thornton C, Yin K K and Admas M J 1996 *J. Phys. D: Appl. Phys.* **29** 424
[19] Batchelor G B and O'Brien R W O 1977 *Proc. Royal Soc. Lond.* **355** 313
[20] Vargas W L and McCarthy J J 2001 *AIChE J.* **47** 1052
[21] Antwerpena W V, Toitb C G D and Rousseaua P G 2010 *Nucl. Eng. Design* **240** 1803
[22] Zhang H W, Zhou Q, Xing H L and Muhlhaus H 2011 *Powder Tech.* **205** 172
[23] Ding Y L, Forster R, Seville J P K and Parker D J 2002 *Powder Tech.* **124** 18
[24] Schlünder E U and Mollekopf N 1984 *Chem. Eng. Process.* **18** 93
[25] Dury C M, Ristow G H, Moss J L and Nakagawa M 1998 *Phys. Rev. E* **57** 4491
[26] Yang R Y, Yu A B, McElroy L and Bao J 2008 *Powder Tech.* **188** 170